Kastamonu Uni., Orman Fakültesi Dergisi, 2022, 22(3): 236-246 Research Article
Kastamonu Univ., Journal of Forestry Faculty
Doi:10.17475/kastorman.1215333

Calculation of Fireline Intensity Using Remote Sensing and Geographic Information Systems: 2021 Milas-Karacahisar Fire

Kadir Alperen COŞKUNER*, Ertuğrul BİLGİLİ

Karadeniz Teknik Universitesi, Faculty of Forestry, Trabzon, 61080, TURKİYE
*Corresponding Author: kacoskuner@ktu.edu.tr

Received Date: 22.04.2022 Accepted Date: 03.08.2022

Abstract

Aim of the study: The objective of this study is to calculate fireline intensity using remote sensing and geographic information systems, to investigate relationship between fireline intensity and VIIRS active fire data, and to develop a practical fireline intensity estimation model.

Material and methods: The Visible Infrared Imaging Radiometer Suite (VIIRS) active fire/hotspot data provided by Suomi National Polar Orbiting Partnership (S-NPP) and National Oceanic and Atmospheric Administration (NOAA-20) satellites were used to estimate the rate of fire spread. Fuel consumption was estimated using Sentinel-2 images, stand type maps and surface and available crown fuel loading models for Turkish red pine (*Pinus brutia* Ten.). The fireline intensity was then calculated using Byram's (1959) fireline intensity equation.

Main results: The results indicated that the number of VIIRS active fire data was well correlated with fireline intensity, rate of fire spread and fuel consumption. The calculated fireline intensity ranged between 175.0 and 47597.2 kW/m with an average value of 9280.4 kW/m. The number of VIIRS active fire data alone explained 72% of the variation in fireline intensity.

Highlights: Satellite based products can be effectively used to calculate fireline intensity through estimating rate of fire spread and fuel consumption easily and effectively in burned areas.

Keywords: Forest fires, VIIRS, Sentinel-2, rate of spread, fuel consumption, fireline intensity

Yangın Şiddetinin Uzaktan Algılama ve Coğrafi Bilgi Sistemleri ile Hesaplanması: 2021 Yılı Milas-Karacahisar Yangını

Öz

Çalışmanın amacı: Bu çalışmanın amacı, uzaktan algılama ve coğrafi bilgi sistemlerini kullanarak yangın şiddetini hesaplamak, yangın şiddeti ile VIIRS aktif yangın verileri arasındaki ilişkiyi araştırmak ve pratik olarak kullanılabilecek bir yangın şiddeti tahmin modeli geliştirmektir.

Materyal ve yöntem: Yangın yayılma oranını tahmin etmek için Suomi Ulusal Kutup Yörünge Ortaklığı (S-NPP) ve Amerikan Ulusal Okyanus ve Atmosfer Dairesi (NOAA-20) uyduları tarafından sağlanan Görünür Kızılötesi Görüntüleme Radyometre Sensöründen (VIIRS) gelen aktif yangın/sıcak nokta verileri kullanılmıştır. Yanıcı madde tüketimini tahmin etmek için Sentinel-2 görüntüleri, meşcere tipi haritaları ve Kızılçam (*Pinus brutia* Ten.) için geliştirilmiş ölü örtü ve tepe yanıcı madde miktarı tahmin modelleri kullanılmıştır. Yangın şiddeti değerleri Byram (1959) tarafından geliştirilen denklemle hesaplanmıştır.

Temel sonuçlar: VIIRS aktif yangın verileri ile yangın şiddeti, yangın yayılma oranı ve yanıcı madde tüketimi arasında anlamlı pozitif korelasyon elde edilmiştir Yangında hesaplanan yangın şiddeti 175.0 ila 47597.2 kW/m arasında değişmiş, ortalama 9280.4 kW/m olarak hesaplanmıştır. Tek başına VIIRS aktif yangın veri sayısı ile yangın şiddetindeki değişimin %72'sini açıklanabilmiştir.

Araştırma vurguları: Uydu tabanlı ürünler, yanan alanlarda yangının yayılma oranı ve yanıcı madde tüketiminin kolay ve etkin bir şekilde tahmin edilmesi yoluyla, yangın şiddetinin hesaplanmasında kullanılabilir.

Anahtar Kelimeler: Orman Yangınları, VIIRS, Sentinel-2, Yangın Yayılma Oranı, Yanıcı Madde Tüketimi, Yangın Şiddeti

Citation (Atıf): Coskuner, K. A., & Bilgili, E. (2022). Calculation of Fireline Intensity Using Remote Sensing and Geographic Information Systems: 2021 Milas-Karacahisar Fire. *Kastamonu University Journal of Forestry Faculty*, 22 (3), 236-246.

Introduction

Fireline intensity is the rate of energy or heat release per unit time per unit length of fire front (Byram, 1959). Fire intensity and fireline intensity can be interchangeably used. The term "fireline intensity" was preferred in this study in accordance with the recent literature (Alexander & Cruz, 2018). Fireline intensity have been used to assess wildland fire's behavior and impacts such as, height of convection column, peak flame temperature, stand mortality, maximum soil temperature, (Alexander & Cruz, 2018) and modeling spot fires (TOVAG, 2011). Therefore, it is a critical component of overall fire management activities (Keeley, 2008). The calculation of fireline intensity requires the estimation of fuel consumption and rate of fire spread and thus must be calculated with an equation (kW/m) (I_B) expressed by Byram (1959) (Eq. 1) as:

$$I_B = H \times w \times r \quad (1)$$

where H is the fuel low heat of combustion (kJ/kg), w is the amount of fuel consumed in the active flaming front (kg/m^2), and r is the linear rate of fire spread (m/s).

Basically, a value of 18700 kJ/kg can be used for the low heat of combustion for fireline intensity (Van Wagner, 1973). Fuel consumption indicates the amount of vegetative biomass consumed during wildland fire (Ottmar, 2014). Fine fuels (needles and branches <0.6 cm in diameter) are considered available fuels (Fernández-Alonso et al., 2013; Küçük & Bilgili, 2007; Küçük et al., 2009; Mitsopoulos & Dimitrakopoulos, 2007) that are consumed in a crown fire (Baysal et al., 2019; Scott & Reinhardt, 2002; Stocks et al., 2004). Fuel consumption can be directly estimated in the field or predicted using models (de Groot et al., 2007; Ottmar, 2014) or satellite data (Andela et al., 2016; Ruecker et al., 2021).

Rate of fire spread refers to the linear rate of advance of a surface head fire, a crown fire, or a backfire (Alexander, 1982). The rate of fire spread should be measured directly in the field or estimated from remotely sensed data. Using remotely sensed data, the rate of fire spread is generally calculated by the distance between fire fronts over an elapsed time period along a line perpendicular to the local fire line (Ruecker et al., 2021). The direction of this line is determined using multispectral airborne data (Ononye et al., 2007) and a handheld infrared camera on a helicopter flying over the fire area (Paugam et al., 2013). Ruecker et al. (2021) followed a similar approach to derive fire rate of spread using the combination of Sentinel-2 images and VIIRS (Visible Infrared Imaging Radiometer Suite) sensor data (mounted on the Suomi National Polar Orbiting Partnership, S-NPP, and National Oceanic and Atmospheric Administration, NOAA-20, satellites). The VIIRS S-NPP dataset is currently available from 20 January 2012 and VIIRS NOAA-20 dataset from 1 January 2020 to the present. Each VIIRS active fire/thermal anomaly location represents the center of a 375m pixel (NASA-FIRMS, 2021). This active fire product has some limitations to detect small scaled (i.e., <1 ha in size) and low intensity fires under tree canopies; however, the detection performance of the product is satisfactory in large scaled and high intensity fires in forested lands (Coskuner, 2022a), and in monitoring and assessing wildfires (Chen et al., 2022; Pinto et al., 2021; Ruecker et al., 2021; Zheng et al., 2021).

The fireline intensity is a product of rate of fire spread and fuel consumption, and is calculated from both field measurements (Bradstock & Auld, 1995; Stocks et al., 2004) and remotely sensed data (Johnston et al., 2017; Ruecker et al., 2021). However, the methods presented in the estimation of fireline intensity using field measurements is labor intensive and time consuming. Satellite based products, on the other hand, can be effectively used to calculate fireline intensity through estimating fire rate of spread and fuel consumption easily and effectively in burned areas.

The objective of this study is to calculate fireline intensity using remote sensing and geographic information systems, to investigate relationship between fireline intensity and VIIRS-based products and develop a practical fireline intensity estimation model. The results of this study will be of some importance in decision making process and overall fire management planning.

Material and Methods

Study Area and Fire Location

The fire records documented by General Directorate of Forestry in Türkiye (GDF) indicated that the fire started at 15:43 local time (UTC+3) within the border of Karacahisar State Forest Enterprise (SFE) in July 31, 2021 and ended in August 11, 2021 at 19:25. The fire was caused by a spark from power lines and affected 12764 ha of forested lands within the border of four SFEs, namely; Karacahisar, Mumcular, Yalı and Çökertme. The burned area is located at 37°01′20 ″N, 27°44′27″ E and at sea level in Milas region, southwestern Türkiye (Figure 1). The average slope is 25-30%.

The region has typical Mediterranean climate with mild short winters and long hot summers. Average annual rainfall is 681.9 mm with precipitation highest in winter and lowest in summer. Average annual air temperature is 18.9 ºC. Turkish red pine (*Pinus brutia* Ten.) was the major tree species dominating the forest canopy prior to fire. Kermes oak (*Quercus coccifera* L.), Terebinth tree (*Pistacia terebinthus* L.), Greek Strawberry-Tree (*Arbutus andrachne* L.), Laurel tree *(Laurus nobilis* L.), *Myrtus communis* L. and *Cistus* spp. Were the common understorey woody species. The altitude varies between 0 and 875 m with an average slope of 27%. The type of soil is brown forest soil.

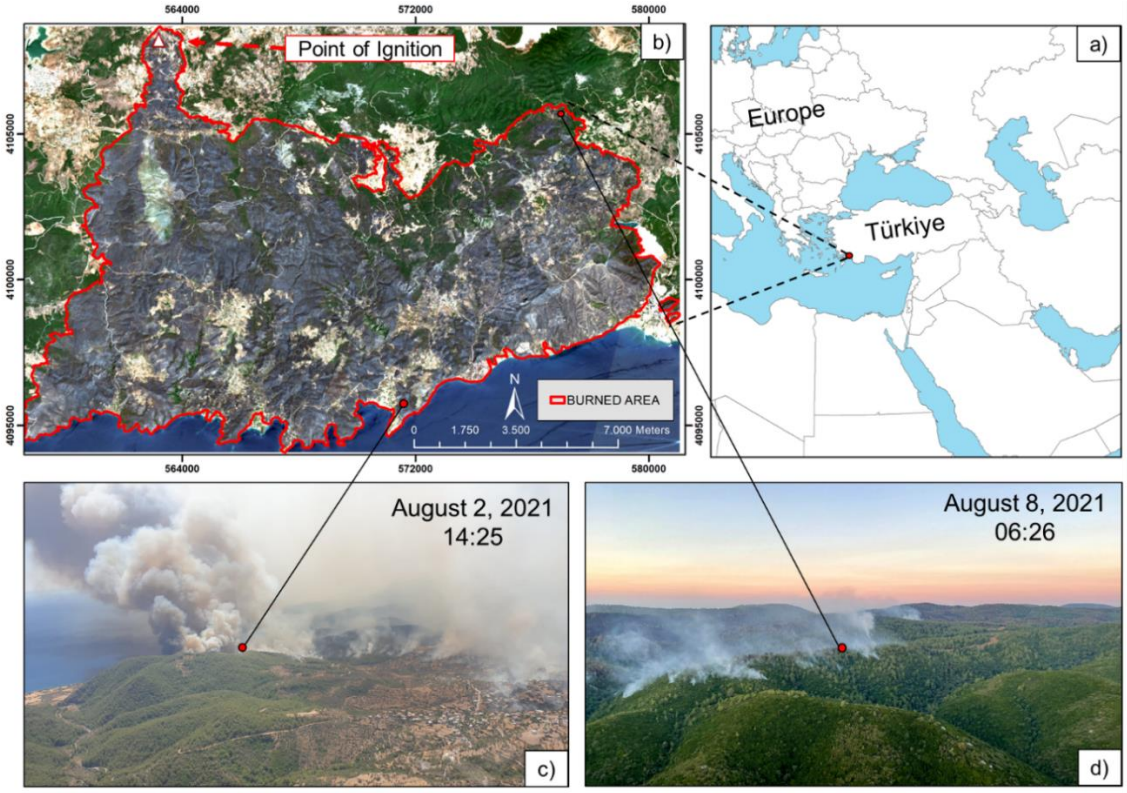

Figure 1. The geographic location of burned area (a, b), and aerial views of fire at 14:25 in August, 2 (~phase 6) (c) and 06:26 in August 8, 2021 (~phase 34) (d).

Estimation of Rate of Fire Spread (ROS)

The rate of fire spread was estimated using the VIIRS active fire/hotspot data provided by Suomi National Polar Orbiting Partnership (VNP14IMGTDL_NRT) and National Oceanic and Atmospheric Administration, formally known as JPSS-1, (VJ114IMGTDL_NRT) satellites (Figure 2a). VIIRS detects active fires. Each active fire detection represents the center of a pixel flagged as containing one or more fires and the pixel size is approximately 375 m. The "location" is the center point of the pixel (Schroeder & Giglio, 2018). Active fire/hotspots were detected at ~ 01:00 - 03:00

am and 13:00-15:00 (UTC+3) by the two satellites for the study area.

The VIIRS active fire/hotspots datasets (FIRMS-NOAA-20, 2021; FIRMS-SUOMI-NPP, 2021) were downloaded for the burned area from NASA - Fire Information for Resource Management System (FIRMS) web platform (NASA-FIRMS, 2021). Detection confidence of VIIRS ranges from 0 to 100%. The nominal and high confident fires (confidence value above 30%) were used in the study.

The rate of fire spread is calculated by the distance between fire fronts over an elapsed time period along a line perpendicular to the local fire line (Ruecker et al., 2021). In this study, the displacement distance to the fire front was measured using the VIIRS active fire data provided by the two satellites. The active fire dataset was divided into phases using the sensing date and time, and the polygons were created using the outer points of each sensing time. The vectors were created in each polygon of phases using an average distance of consecutive phases (Figure 2b). Average distance was determined from three measurements of displacement distance. Then, the estimated rate of fire spread was calculated for each phase by dividing the average distances between fire fronts by the time elapsed between the overpasses of the two satellites over the burning area.

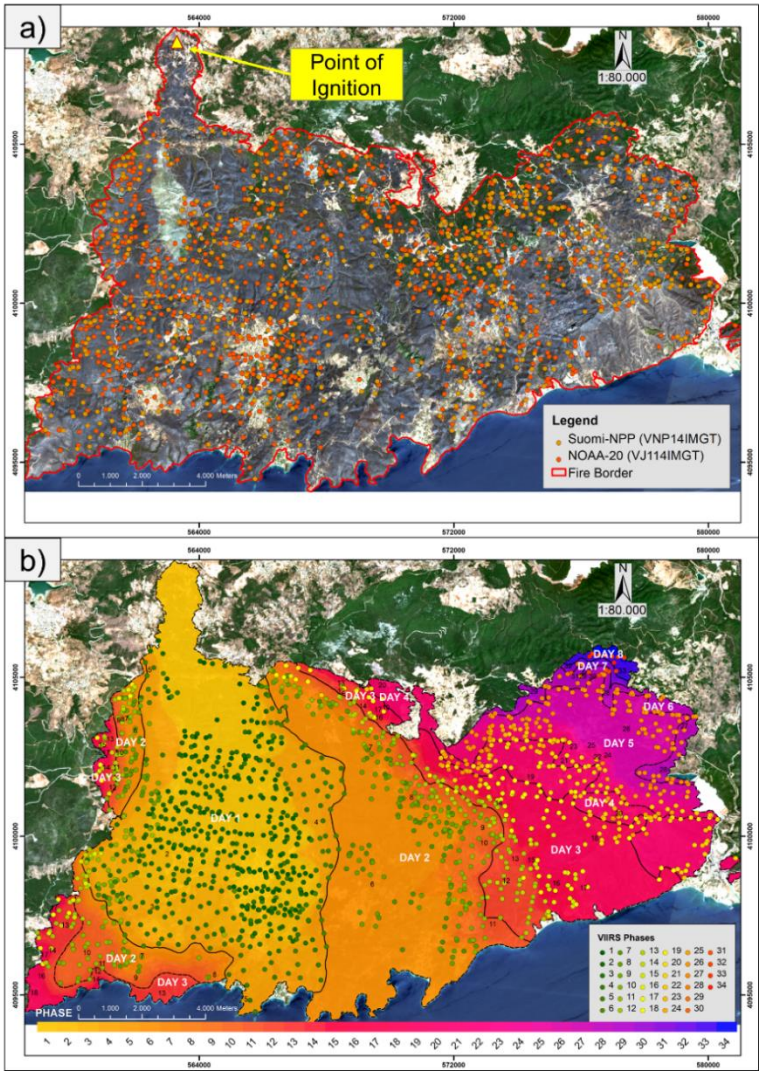

Figure 2. The Sentinel-2B images (August 15, 2021) of burned area (a). The fire was divided into 34 phases between July 31 and August 8 in 2021(b). The filled circles (a) correspond to the detections of VIIRS fire/hotspot by SUOMI-NPP and NOAA-20 satellites from August 1 at 02:16 am and August 8 at 03:26, and phases of detections (b) for the burned area.

Calculation of Fuel Consumption

Forest stand type maps were used for the surface and crown fuel load calculation for the burned area (Figure 3a). These maps were generated from stereo interpretation of aerial photographs and field inventory data. Since, mostly the fine fuels are consumed in a crown fire (Scott & Reinhardt, 2002; Stocks et al., 2004) involving needles and branches <0.6 cm in diameter are consumed in a crown fire, surface (fine fuel - duff) (SFL) and available crown fuel loading (CFL) (needles and branches <0.6 cm in diameter) were calculated.

The forest stand type maps include tree species, development stage and crown closure of the stands. Tree characteristics and fuel models developed for surface fuel loading for Turkish red pine (*Pinus brutia*) (TOVAG, 2011) were used in this study. The models use stand characteristics of Turkish red pine as inputs such as stage of stand development and crown closure. Available crown fuel loading of Turkish red pine stands was predicted using the models developed by Baysal (2021). Surface and available CFL for the stands were calculated using mean tree diameter of the stand and stand density (#trees/ha). The available CFL and calculated SFL (in kg/m^2) values were then used in the analyses.

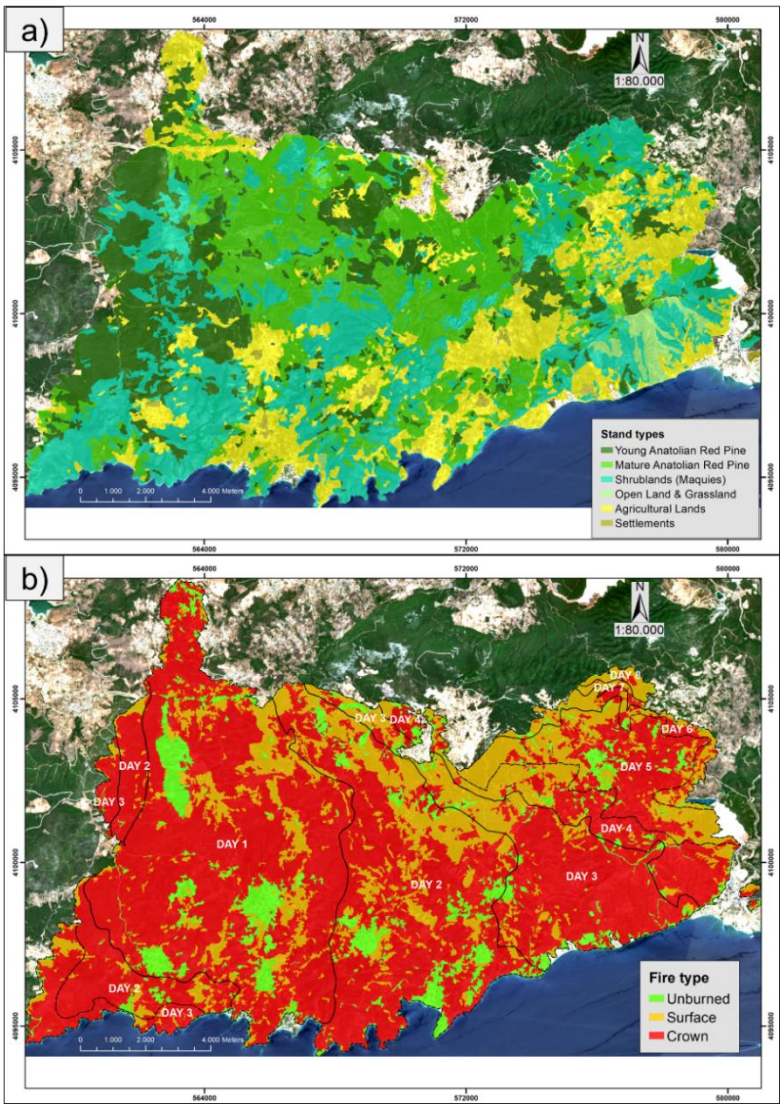

Figure 3. Forest stand type map of the burned area (a) and fire type classes after the supervised image classification of Sentinel-2B TCI images (b).

Burned area was assessed using the Sentinel-2B satellite images. Satellite images were obtained from Copernicus Open Access Hub portal (https://scihub.copernicus.eu). Pre- (July 23, 2021) and post-fire (August 15, 2021) images of the study area were selected as close to fire occurrence day as possible. The supervised image classification method was performed to define the actual burned area calculation for the study area. The three fire type classes namely; *i*) Unburned *ii*) Surface fire and *iii*) Crown fire were created using the True Color Images (TCI) of Sentinel-2B at 10 m spatial resolution (Figure 3b).

To classify fire type classes, the Maximum Likelihood Classification tool was used in Spatial Analyst extension in ArcGIS software (ArcGIS® v. 10.2). The classified fire type raster layer was converted into shape file polygon layer, and then intersected with the stand type layer. To calculate the fuel consumption, both the available CFL and SFL were assumed to be consumed in crown fire class, and only SFL in surface fire class. The total fuel consumption (kg) was then calculated for each fire phase and converted into kg/m^2. Fireline intensity calculations require that fuel consumption be given in kg/m^2.

Fireline Intensity Calculation and Statistical Analysis

The Byram's fireline (I_B) intensity was calculated using a low heat of combustion, estimated rate of fire spread and fuel consumption for each fire phase (Byram, 1959) (1). The flowchart of fire intensity calculation is given in Figure 4.

Pearson correlation and nonlinear regression analyses were conducted to study the relationship between the number of VIIRS active fire data and associated variables. All statistical analyses were conducted using SPSS 26.0 for Windows (SPSS, 2019).

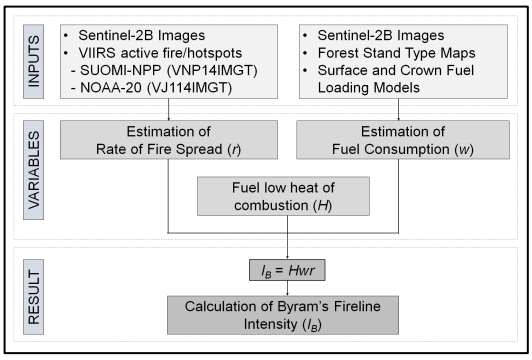

Figure 4. The flowchart of the calculation of Byram's fireline intensity using remote sensing and fuel data.

Results

The VIIRS fire data indicated that a total of 1527 active fire/hotspot (nominal and high confidence) were detected from August 1 to 8 in the study area. Of these data, 643 active fires were detected by SUOMI-NPP, and 884 fires were detected by NOAA-20 satellite. The fire was divided into 34 phases using the detection time of these satellites (Figure 2). The number of VIIRS active fire data varied from 1 to 169 with an average of 45 detections in each fire phase (Table 1).

Table 1. Descriptive statistics of the data used and calculated during August 1-8, 2021 in Milas-Karacahisar Fire.

Variables	Mean	SE	Max	Min
Number of VIIRS Hotspots	44.9	38.4	169.0	1.0
Crown Fire Ratio (%)	51.9	20.3	82.5	10.3
Rate of Fire Spread (m/min)	4.9	5.4	23.5	0.1
Fuel Consumption (kg/m^2)	5.9	0.8	7.6	3.9
Fireline Intensity (kW/m)	9280.4	11123.1	47597.2	175.0

The results of the supervised classification of the Sentinel-2B images of the burned area indicated that a total of 15791.4 ha land area (including agricultural fields and grasslands) was affected. Of these, 11840.3 ha (74.9 %) was crown, and 4131.1 ha (24.1%) was surface fire. The crown fire ratio varied between 10.3 and 82.5% with an average 51.9% in fire phases (Table 1).

The rate of fire spread varied between 0.1 and 23.5 m/min with an average 4.9 m/min, and the fuel consumption varied between 3.9

and 7.6 kg/m^2 with an average 5.9 kg/m^2 in fire phases. The calculated fireline intensity varied between 175.0 and 47597.2 kW/m with an average 9280.4 kW/m in fire phases (Table 1). The time series of fire line intensity is given in Figure 5.

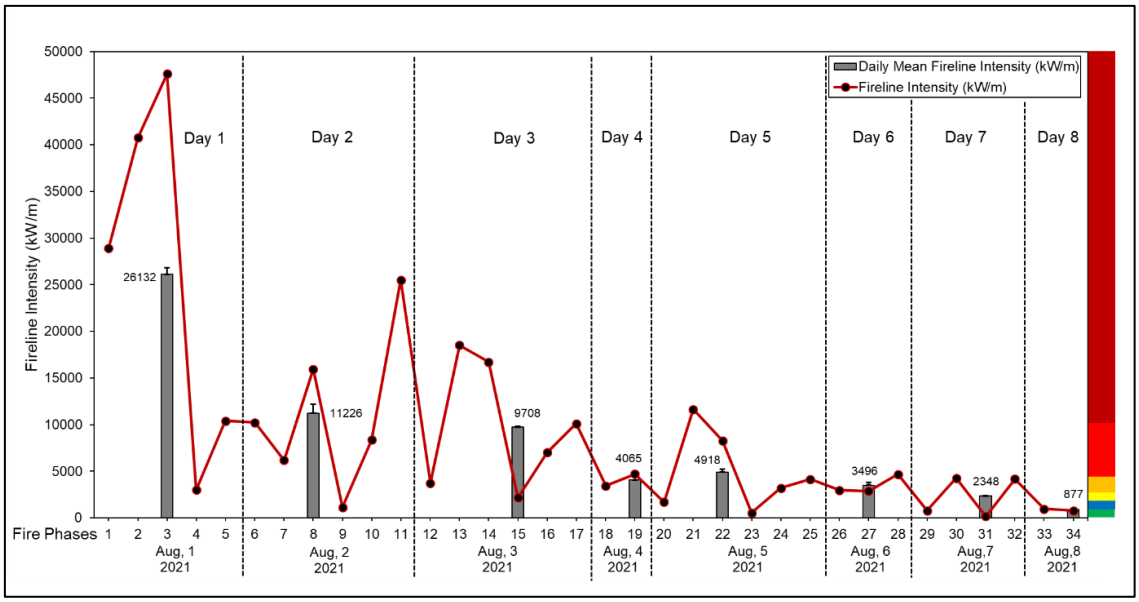

Figure 5. Time series of calculated fireline intensity in phases, and daily means in the Milas-Karacahisar Fire. Colored bar on the right side indicates fireline intensity classes of Canadian Fire Danger Rating system (Cole & Alexander, 1995).

Correlation analysis was undertaken to determine the relationship between the number of VIIRS active fire data and associated variables. The correlation analysis indicated that the number of VIIRS active fire data was positively correlated with crown fire ratio (r=0.590, p<0.01), rate of fire spread (r=0.764, p<0.01), fuel consumption (r=0.454, p<0.01) and fireline intensity (r=0.784, p<0.01). There was also a positive correlation between crown fire ratio and fireline intensity (r=0.416, p<0.05) (Table 2).

Table 2. Pearson correlation matrix for number of VIIRS active fire data and associated variables.

Variables	Number of VIIRS Hotspots	Crown Fire Ratio (%)	Rate of Fire Spread (m/min)	Fuel Consumption (kg/m^2)	Fireline Intensity (kW/m)
Number of VIIRS Hotspots	1				
Crown Fire Ratio (%)	0.590**	1			
Fire Rate of Spread (m/min)	0.764**	0.400*	1		
Fuel Consumption (kg/m^2)	0.454**	0.434*	0.485**	1	
Fireline Intensity (kW/m)	0.784**	0.416*	0.995**	0.543**	1

*Correlation is significant at the 0.05 level (2-tailed).**Correlation is significant at the 0.01 level (2-tailed)

One of the main objectives of the study was to predict fireline intensity using remote sensing data, only for practical purposes. The nonlinear regression analysis was performed to predict fireline intensity using the number of VIIRS hotspot data as an input. The results indicated that the number of VIIRS alone explained 72% of the variation in fireline intensity (kW/m) (Eq. 2) (Figure 6).

$$\text{Fireline intensity} = 2563.4 + 43.072 \times (\text{VIIRS}) + 1.3694 \times (\text{VIIRS})^2 \qquad (R^2 = 0.72) \qquad (2)$$

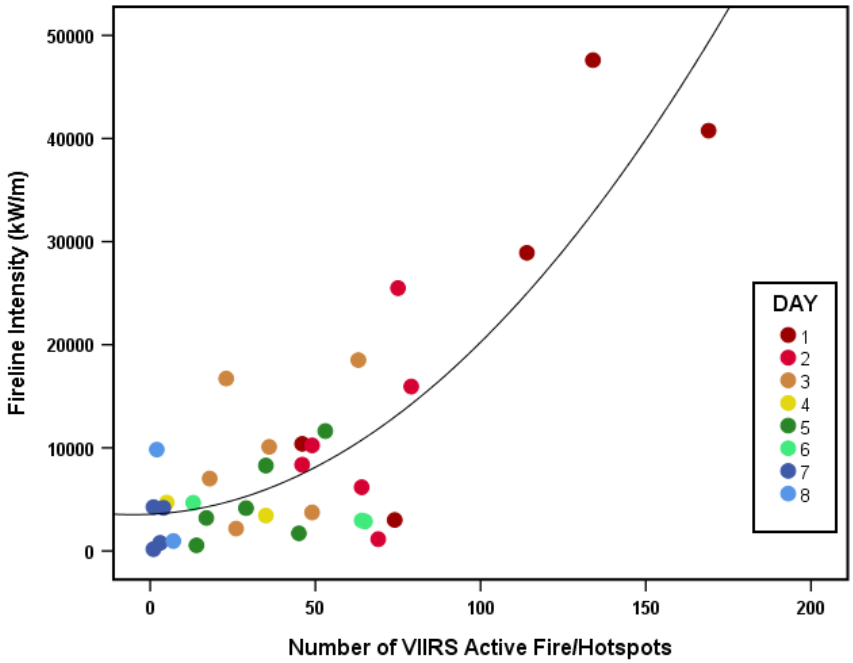

Figure 6. The relationship between the number of VIIRS active fire detection and fireline intensity over one satellite overpass. The colored circles indicate the days from July 31 to August 8, 2021.

Discussion

This study investigates the relationship between fireline intensity and VIIRS active fire/hotspot data. To calculate fireline intensity, rate of fire spread and fuel consumption were estimated. The rate of fire spread was directly estimated with satellite remote sensing observations using 375 m resolution VIIRS active fire data. VIIRS has been used for mapping of burned areas (Pinto et al., 2021; Urbanski et al., 2018) and for the prediction of rate of fire spread (Pinto et al., 2016; Ruecker et al., 2021). VIIRS active fire data has the highest spatial resolution in the available cost-free fire products (Sofan et al., 2020). Although VIIRS has some limitations to detect small scaled (<1 ha in size) and lower intensity fires especially under tree canopies; however, the detection performance of the product is satisfactory in large scaled and intense fires in forested lands (Coskuner, 2022a). Large fires such as Milas-Karacahisar Fire with high fireline intensity, fire severity and long fire duration provide better detection opportunities for satellite based fire products (Fusco et al., 2019). Therefore, VIIRS data could be effectively used for fire control and the assessment of fire effects in large scaled wildfires.

The VIIRS active fire data indicated that the Milas-Karacahisar fire moved from north to south reaching the Aegean Sea in the first day of the fire. The fire spread was from southwest to northeast in the following days, and the detection of hotspots ended in August 1, 2021 (Figure 2b). The estimated rate of fire spread varied between 0.1 and 23.5 m/min with an average 4.9 m/min in the fire (Table 1). High values of the estimated rate of fire spread (23.5 m/min) (Figure 2b) and fireline intensity (47597.2 kW/m) (Figure 5) indicate extreme fire events. These kinds of fires are considered as “explosive” or “super critical” and the characteristics of fires commonly associated with extreme fire behavior (e.g., rapid spread rates, medium to long range spotting, continuous crown fire development, massive convection columns, fire whirls,) is a certainty (Figure 1c) (Cole & Alexander, 1995).

The correlation analysis indicated that the number of VIIRS active fire/hotspots were positively correlated with crown fire ratio, rate of fire spread, fuel consumption and fireline intensity (p<0.01, Table 2). The number of VIIRS active fires explained 72% variation in the fireline intensity in Milas-Karacahisar fire (Equation 2, Figure 6). One of the objectives of this study was to provide

fire managers with a practical tool to evaluate fire potential and the effectiveness of fire suppression activities through estimating fireline intensity.

The fuel load was predicted using the forest management stand type maps with the surface (TOVAG, 2011) and available crown fuel loading (Baysal, 2021) models of Turkish red pine. The stand type maps are usually produced from the stereo interpretation of aerial photographs and field inventory data, thus, the spatial resolution is high. However, the temporal resolution of these maps are up to 20 years and they reflect the inventory year they were made. The quick change in vegetation dynamics in Turkish red pine stands and in Mediterranean shrubland communities (maquies) through anthropogenic (i.e., silvicultural treatments, fires) and natural (i.e., wind - storm damages) disturbances affects stand characteristics thereby leading to changes in actual fuel loads (Coskuner, 2022b). Timely, accurate and easily available information on actual fuel loads are of significant importance in fire management (Coskuner, 2022b; Yavuz et al., 2018). Therefore, in this regard, remote sensing applications with high spatial and temporal resolution could be effectively used. Some case studies are already available, utilizing a combination of remote sensing data and field work to estimate fuel load in the Mediterranean basin (Mallinis et al., 2013), but national level satellite based fuel type and load estimation is also needed. To this end, Sentinel-2 satellite data with high spatial (10-60 m) and temporal (~10 days) resolution may be of great use for fuel mapping, and there are some initiatives for fuel mapping with Sentinel-2 data in the Mediterranean basin (Stefanidou et al., 2020) at the national scale. New studies should be initiated to develop tools for fuel mapping utilizing satellite images and other modern inventory technologies.

Conclusion

In this study, the rate of fire spread and fuel consumption was estimated using the VIIRS active fire data and Sentinel-2B images, and fireline intensity was calculated for Milas-Karacahisar fire of 2021 affecting nearly 16 thousand hectares of land area. The fire was divided into 34 phases covering 31 July to 8 August by active fire detection day and time using fire detection data from VIIRS sensors in S-NPP and NOAA-20 satellites. The results showed that the fire fireline intensity reached up to 47597.2 kW/m in Milas-Karacahisar fire.

The number of VIIRS active fire data points was well correlated with crown fire ratio, fire rate of spread, fuel consumption and fireline intensity, and explained 72% variation in the fireline intensity. Fuel consumption was estimated using forest stand type maps with surface and available crown fuel loading of Turkish red pine stands. Thanks to the stereo interpretation of the aerial photographs, the spatial resolution of the maps produced is high. However, these maps can only reflect the situation of fuel conditions when these maps were produced. Moreover, they were produced for forest management activities and they rarely include the information necessary for fuel load assessment.

Acknowledgements

The data was obtained from NASA's Fire Information for Resource Management System (FIRMS) (https://earthdata.nasa.gov/firms), part of NASA's Earth Observing System Data and Information System (EOSDIS). The authors also would like to acknowledge the help of Mugla Regional Forest Directorate and Murat Bozturk for providing forest management field inventory data for the present study.

Ethics Committee Approval

N/A

Peer-review

Externally peer-reviewed.

Author Contributions

Conceptualization: K.A.C.; Investigation: K.A.C.; Material and Methodology: K.A.C.; Supervision: K.A.C. and E.B.; Visualization: K.A.C.; Writing-Original Draft: K.A.C. and E.B.; Writing-review & Editing: K.A.C. and E.B. All authors have read and agreed to the published version of manuscript.

Conflict of Interest

The authors have no conflicts of interest to declare.

Funding

The authors declared that this study has received no financial support.

References

Alexander, M.E. (1982). Calculating and Interpreting Forest Fire Intensities. *Canadian Journal of Botany-Revue Canadienne De Botanique*, 60(4), 349-357.

Alexander, M.E., & Cruz, M.G. (2018). Fireline Intensity. In S. L. Manzello (Ed.), Encyclopedia of Wildfires and Wildland-Urban Interface (WUI) Fires, Springer International Publishing, 1-8.

Andela, N., van der Werf, G. R., Kaiser, J. W., van Leeuwen, T. T., Wooster, M. J., & Lehmann, C. E. R. (2016). Biomass burning fuel consumption dynamics in the tropics and subtropics assessed from satellite. *Biogeosciences*, 13(12), 3717-3734.

Baysal, I. (2021). Vertical Crown Fuel Distributions in Natural Calabrian Pine (Pinus brutia Ten.) Stands. *Croatian Journal of Forest Engineering*, 42(13), 301-312.

Baysal, İ., Yurtgan, M., Küçük, Ö., & Öztürk, N. (2019). Estimation of Crown Fuel Load of Suppressed Trees in Non-treated Young Calabrian Pine (Pinus brutia Ten.) Plantation Areas. *Kastamonu University Journal of Forestry Faculty*, 19(3), 350-359.

Bradstock, R.A., & Auld, T.D. (1995). Soil Temperatures During Experimental Bushfires in Relation to Fire Intensity: Consequences for Legume Germination and Fire Management in South-Eastern Australia. *Journal of Applied Ecology*, 32(1), 76-84.

Byram, G.M. (1959). Combustion of forest fuels. In K. P. Davis (Ed.), *Forest Fire: Control and Use*, MCGraw-Hill, 61-89.

Chen, J., Li, R., Tao, M., Wang, L.T., Lin, C., Wang, J., . . . Chen, L. (2022). Overview of the performance of satellite fire products in China: Uncertainties and challenges. *Atmospheric Environment*, 268, 118838.

Cole, F.V., & Alexander, M.E. (1995). Head fire intensity class graph for FBP System Fuel Type C-2 (Boreal Spruce). Alaska Department of Natural Resources, Division of Forestry, Fairbanks, AK and Natural Resources Canada, Canadian Forest Service, Edmonton, AB.

Coskuner, K.A. (2022a). Assessing the performance of MODIS and VIIRS active fire products in the monitoring of wildfires: a case study in Turkey. *iForest - Biogeosciences and Forestry*, 15(2), 85-94.

Coskuner, K.A. (2022b). Land use/land cover change as a major driver of current landscape flammability in Eastern Mediterranean region: A case study in Southwestern Turkey *Bosque (Valdivia)*, 43(2), 157-167.

de Groot, W.J., Landry, R., Kurz, W., Anderson, K., Englefield, P., Fraser, R., . . . Pritchard, J. (2007). Estimating direct carbon emissions from Canadian wildland fires. *International Journal of Wildland Fire*, 16, 593–606.

Fernández-Alonso, J.M., Alberdi, I., Álvarez-González, J.G., Vega, J.A., Cañellas, I., & Ruiz-González, A.D. (2013). Canopy fuel characteristics in relation to crown fire potential in pine stands: analysis, modelling and classification. *European Journal of Forest Research*, 132(2), 363-377.

FIRMS-NOAA-20. (2021). NRT VIIRS 375 m Active Fire product VJ114IMGTDL_NRT distributed from NASA FIRMS. Available on-line [https://earthdata.nasa.gov/firms]. 10.5067/FIRMS/VIIRS/VJ114IMGT_NRT.002.

FIRMS-SUOMI-NPP. (2021). NRT VIIRS 375 m Active Fire product VNP14IMGT distributed from NASA FIRMS. Available on-line [https://earthdata.nasa.gov/firms]. doi:10.5067/FIRMS/VIIRS/VNP14IMGT_NRT.002

Fusco, E.J., Finn, J.T., Abatzoglou, J.T., Balch, J.K., Dadashi, S., & Bradley, B.A. (2019). Detection rates and biases of fire observations from MODIS and agency reports in the conterminous United States. *Remote Sensing of Environment*, 220, 30-40.

Johnston, J.M., Wooster, M.J., Paugam, R., Wang, X.W., Lynham, T.J., & Johnston, L.M. (2017). Direct estimation of Byram's fire intensity from infrared remote sensing imagery *International Journal of Wildland Fire*, 26(8), 668-684.

Keeley, J.E. (2008). Fire. In S. E. Jørgensen & B. D. Fath (Eds.), *Encyclopedia of Ecology* (pp. 1557-1564). Academic Press.

Küçük, Ö., & Bilgili, E. (2007). Crown Fuel Load for Young Calabrian Pine (Pinus brutia Ten.) Trees. *Kastamonu University Journal of Forestry Faculty*, 7(2), 180-189.

Küçük, Ö., Bilgili, E., Durmaz, B.D., Sağlam, B., & Baysal, İ. (2009). Örtü Yangınının Tepe Yangınına Geçişinde Etkili Olan Faktörler. *Kastamonu University Journal of Forestry Faculty*, 9(2), 80-85.

Mallinis, G., Mitsopoulos, I., Stournara, P., Patias, P., & Dimitrakopoulos, A.P. (2013). Canopy Fuel Load Mapping of Mediterranean Pine

Sites Based on Individual Tree-Crown Delineation. *Remote Sensing*, 5(12), 6461-6480.

Mitsopoulos, I.D., & Dimitrakopoulos, A.P. (2007). Canopy fuel characteristics and potential crown fire behavior in Aleppo pine (Pinus halepensis Mill.) forests. *Annals of Forest Science*, 64(3), 287-299.

NASA-FIRMS. (2021). Fire Information for Resource Management System (FIRMS), Active Fire Data.

Ononye, A.E., Vodacek, A. & Saber, E. (2007). Automated extraction of fire line parameters from multispectral infrared images. *Remote Sensing of Environment*, 108(2), 179-188.

Ottmar, R.D. (2014). Wildland fire emissions, carbon, and climate: Modeling fuel consumption. *Forest Ecology and Management*, 317, 41-50.

Paugam, R., Wooster, M.J., & Roberts, G. (2013). Use of Handheld Thermal Imager Data for Airborne Mapping of Fire Radiative Power and Energy and Flame Front Rate of Spread. *IEEE Transactions on Geoscience and Remote Sensing*, 51(6), 3385-3399.

Pinto, M.M., Trigo, R.M., Trigo, I.F., & DaCamara, C. C. (2021). A Practical Method for High-Resolution Burned Area Monitoring Using Sentinel-2 and VIIRS. 13(9), 1608.

Pinto, R., Benali, A., Sá, A., Fernandes, P., Soares, P.M.M., Cardoso, R., . . . Pereira, J.F. (2016). Probabilistic fire spread forecast as a management tool in an operational setting. *SpringerPlus*, 5, 1205.

Ruecker, G., Leimbach, D., & Tiemann, J. (2021). Estimation of Byram's Fire Intensity and Rate of Spread from Spaceborne Remote Sensing Data in a Savanna Landscape. *Fire*, 4(4), 65.

Schroeder, W., & Giglio, L. (2018). *NASA* VIIRS Land Science Investigator Processing System (SIPS) Visible Infrared Imaging Radiometer Suite (VIIRS) 375 m & 750 m Active Fire Products. Product User's Guide Version 1.4, NASA. 23p.

Scott, J.H., & Reinhardt, E.D. (2002). Estimating canopy fuels in conifer forests. *Fire Management Today*, 62, 45-50.

Sofan, P., Bruce, D., Schroeder, W., Jones, E., & Marsden, J. (2020). Assessment of VIIRS 375 m active fire using tropical peatland combustion algorithm applied to Landsat-8 over Indonesia's peatlands. *International Journal of Digital Earth*, 13(12), 1695-1716.

SPSS, I.C. (2019). IBM SPSS Statistics for Windows, Version 26.0. In IBM Corp.

Stefanidou, A., Gitas, I. Z., & Katagis, T. (2020). A national fuel type mapping method improvement using sentinel-2 satellite data. *Geocarto International*, 1-21.

Stocks, B.J., Alexander, M.E., Wotton, B.M., Stefner, C.N., Flannigan, M.D., Taylor, S.W., . . . Lanoville, R.A. (2004). Crown fire behaviour in a northern jack pine black spruce forest. *Canadian Journal of Forest Research*, 34(8), 1548-1560.

TOVAG. (2011). Towards Turkish National Fire Danger Rating System. Part 1: Fire Behavior Prediction System (TOVAG 108O327). The Scientific and Technological Research Council of Türkiye (TUBITAK). Project Report, 89p. TUBITAK.

Urbanski, S., Nordgren, B., Albury, C., Schwert, B., Peterson, D.L., Quayle, B., & Hao, W.M. (2018). A VIIRS direct broadcast algorithm for rapid response mapping of wildfire burned area in the western United States. *Remote Sensing of Environment*, 219, 271-283.

Van Wagner, C.E. (1973). Height of Crown Scorch in Forest Fires. *Canadian Journal of Forest Research,* 3(3), 373-378.

Yavuz, M., Sağlam, B., Küçük, Ö., & Tüfekçioğlu, A. (2018). Assessing forest fire behavior simulation using FlamMap software and remote sensing techniques in Western Black Sea Region, Turkey. *Kastamonu University Journal of Forestry Faculty*, 18(2), 171-188.

Zheng, Y., Liu, J., Jian, H., Fan, X., & Yan, F. (2021). Fire Diurnal Cycle Derived from a Combination of the Himawari-8 and VIIRS Satellites to Improve Fire Emission Assessments in Southeast Australia. 13(15), 2852.